To be submitted to a refereed journal after document review clearance.

Metrology gauges for spatial interferometry

Yekta Gürsel

Jet Propulsion Laboratory
California Institute of Technology
4800 Oak Grove Dr., Pasadena, CA 91109

ABSTRACT

Heterodyne interferometers have been commercially available for many years. in addition, many versions have been built at JPL for various projects. This activity is aimed at improving the accuracy of such interferometers from the 1-30 nanometer level to the picometer level for use in the proposed Stellar Interferometry Mission (SIM) as metrology gauges. In the null-gauge configuration, we obtained a precision of 0.6 picometers at time scales of 2,500 seconds. In the relative-gauge configuration, we obtained an accuracy of 0.13 picometers rms in vacuum at time scales of few minutes, using a better constructed instrument with higher signal to noise ratio.

1. INTRODUCTION

The Stellar Interferometry Mission (SIM) requires metrology interferometers with a relative accuracy of 1-2 root-]nmm-squared (rms) picometers to attain its design goals. In the current design, these interferometers are one-long-arm, heterodyne interferometers which monitor the distance between two fiducials.

Two different implementations of the basic gauge architecture have been examined. The null-gauge experiment determines the ultimate precision of heterodyne interferometers by using two of these with spatially coincident beams. The relative-gauge experiment determines the extent of systematic errors which are absent in the! null configuration by measuring small distances (few wavelengths of light) from a given set point.

The descriptions of these experiments were first published in two SPIE proceedings[4 5] This paper combines the results published in these proceedings and introduces the next step in linear metrology, namely auto-aligning, 3-dimensional, picometer metrology gauge [6].

2. NULL METROLOGY G AUGE

The null-metrology gauge consists of two heterodyne interferometers with spatially coincident light paths. As our vacuum chamber had not yet been delivered at the time this experiment was performed, we chose this scheme to eliminate the effect of the density fluctuations in air which limit the accuracy of the interferometers to ~10 nanometers rms. One of the interferometers is used to servo the distance being monitored to the null of the interferometer, while the other interferometer is used as a read-out device.

The schematic layout of the experiment is shown in Fig. 1. The light from a frequency-stabilized He-Ne laser impinges on a 45 degree linear polarizer. The light from the output of the polarizer is separated into two orthogonal polarizations (S and 1') by a suitably placed polarizing beam splitter. Each of these polarizations is then routed through an acousto-optic modulator.

These modulators are driven by CB radios with a frequency difference of 10 kHz. The frequency shifted beams are then recombined by another polarizing beam splitter. The recombined beam is sent through a pin-hole assembly to spatially filter tile beam. The spatial filtering also makes the output beam insensitive to the directional fluctuations of the input beam.

A small part of this beam is then diverted into a 45 degree polarizer and a photodiode which acts a reference detector. The rest of the beam enters a bealn-launcher assembly which consists of a polarizing beam splitter and two quarter-wave plates. Half of the beam directly passes through the polarizing beam splitter and strikes the

Figure 1: The Null Metrology Gauge

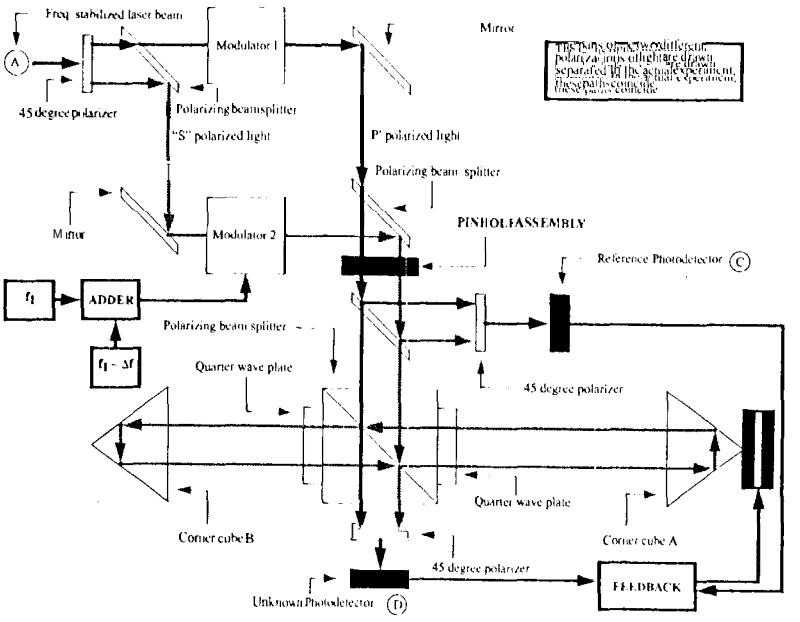

photodetector after passing through a 45 degree polarizer. The other half of the beam maim a round trip between the corner cubes and exits the inter'feromctcr coincident with the first half of the beam and hits the photodetector after passing through the same polarizer. The corner cubes are separated by a nominal distance of ~ 75 cm.

The relative phase of the signal coming out of the latter photodetector (the unknown photodetector) with respect to the phase of the signal coming out of the reference detector is directly a measure of the distance between the two corner cubes. In effect, the heterodyne interferometer converts an actual path-length change of one light wavelength into a phase change of one cycle of a sinusoidal wave at a frequency equal to the difference between the two driving frequencies of the acousto-optic modulators 3

The set-u~) as described above consists of a single heterodyne interferometer. In order to place another interferometer which has very-llearly-ttl[:-salr]c optical path, we added another driving signal to one of the modulators. The frequency of this driving signal is 20 kHz more than the frequency of the signal applied to the other modulator.

In this case, the outputs of the reference and the unknown photodetectors contain 3 signals at the frequencies of 10 kHz, 20 kHz and 30 kHz. The 10 kHz and the 20 kHz signals are separated from each other and the 30 kHz signal by an assembly of notch filters which also perform some 120 Hz hum rejection to enable us to work under normal lighting without saturating the amplifiers.

These sinusoidal signals are amplified and converted iuto square-v'avc signals by a post-amplifier circuit consisting of filters and comparators. The square-wave signals arc then fed into a phase digitizer which digitizes the relative phase of the 10 kHz unknown, 20 kHz reference and the 20 kHz unknown signals with respect to the phase of the 10 kHz reference signal.

The relative phase signal from the 10 kHz interferometer is digitally processed and converted back into au analog feedback signal which is applied to a piezo-electric transducer. This transducer translates one of the corner cubes to hold the 10 kHz interferometer at null.

The relative phase signals from both interferometers are digitally recorded on a magnetic disk during the experiment. The data are analyzed after the recording is completed.

The results of various ruus between March 18, 1992 and April 23, 1992 are shown in Fig. 2. The Allan deviation (square root of Allan variance) of the difference between the 10 kHz and the 20 kHz interferometer signals is plotted as a function of the integration time. The curve which has the largest overall Allan deviation is plotted using our first data. The curve which has the lowest overall Allan deviation was plotted using data taken 011 April 23, 1992.

Figure 2: Null metrology results

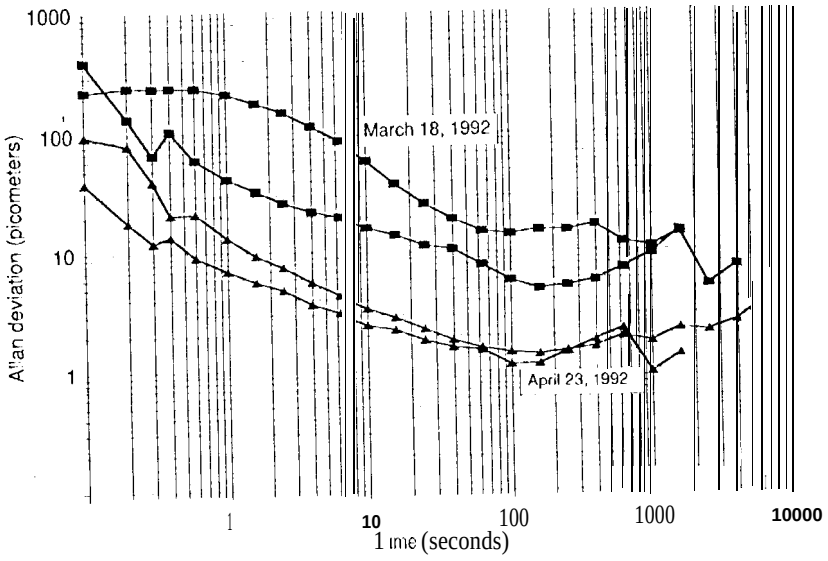

The reason for the dramatic improvement was the elimination of scattered light reflected back towards the laser. The servo system had also been improved during that time which lowered the low-integration-time parts of the curve. The best result using this configuration was a difference deviation of 1.3 picometers at an integration time of 100 seconds. The curve then slowly rose to 2 picometers at integration times close to 4,000 seconds.

We determined the cause of the upward drift at long integration times to be the temperature sensitivity Of the electronic circuits which amplify and shape the analog signals. As the data were being taken, the drifting room temperature caused the various Components in the electronics circuits to drift. Since the 10 kHz and the 20 kHz interferometers used different sets of electronics, a time varying phase difference was introduced because of the small differences between the circuits due to component tolerances.

To reduce the effect of this temperature related slow drift, we constructed a switching network which swapped the entire sets of amplifier and shaping circuits between the interferometers at regular intervals (30 sec). The circuits were also upgraded using low temperature coefficient, precision components.

The results of these modifications is shown in Fig. 3. As a reference, the Allan deviation from the April 11, 1992 data is also shown. The new data give an Allan deviation for the difference signal between the interferometers which reaches down to 0.6 picometers at integration times of 2,500 seconds aud it stays under 2 picometers at integration times Of 10,000 seconds.

3. RELATIVE METROLOGY GAUGE

The relative metrology gauge consists of two heterodyne interferometers with spatially separated paths as shown in Fig. 4 and Fig. 5. Since the physical laser beams do not overlap, each acousto-optic modulator is driven with a single frequency. The frequency difference between the drives to the acousto-optic modulators is 10 kHz. One of the interferometers is used to servo the distance between the corner cubes to a slowly varying separation, while the other interferometer is used as a read-out device.

The relative metrology experiment is designed to classify and eliminate various sources of systematic errors which arc absent in a null-metrology gauge. The polarization leakage caused by several imperfect optical elements (Fig. G) causes a systematic error at the output of the interferometer which is a periodic function of the distance between the corner cubes with a period of exactly one wavelength. The amplitude of this systematic error could be as large as 10 nanometers.

Figure 3: Null metrology with electronic switching

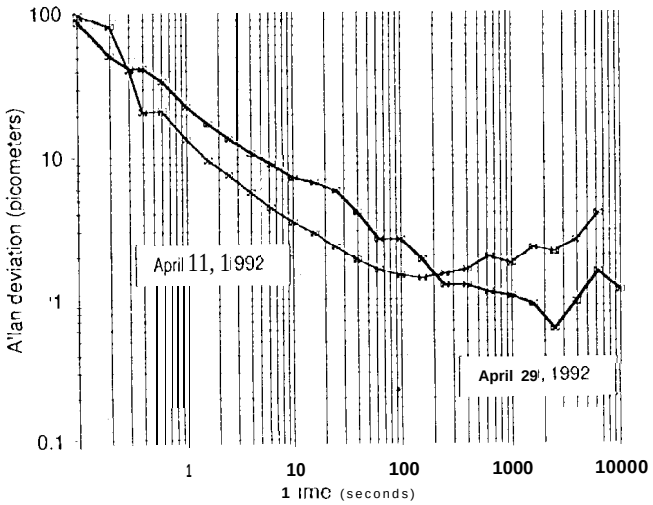

Figure 4: Relative metrology interferometer (a)

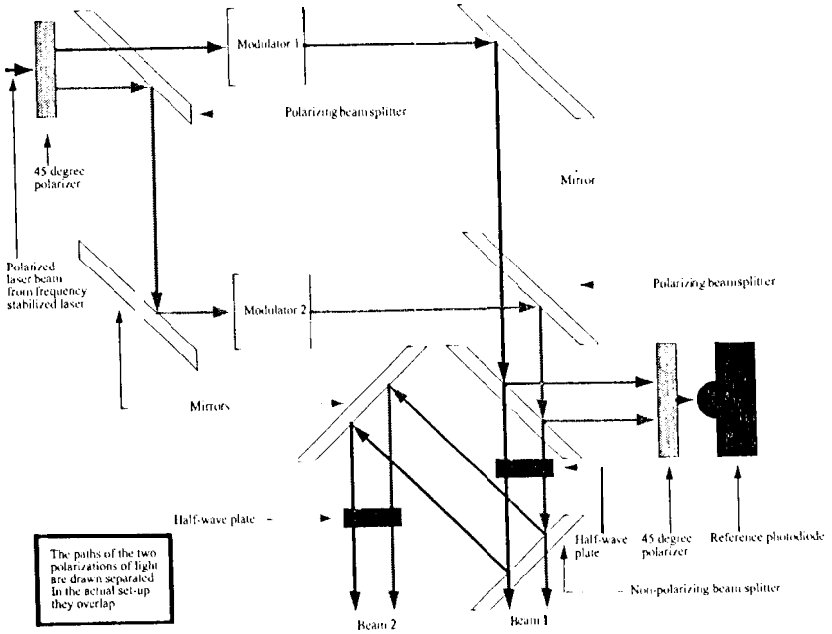

Figure 5: Relative metrology interferometer (b)

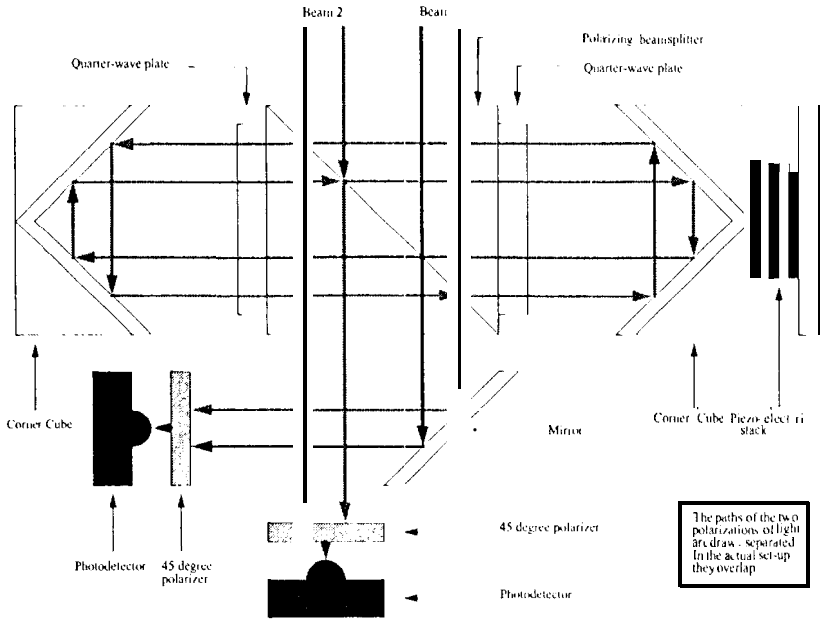

Figure 6: Polarization leakage (self-interference)

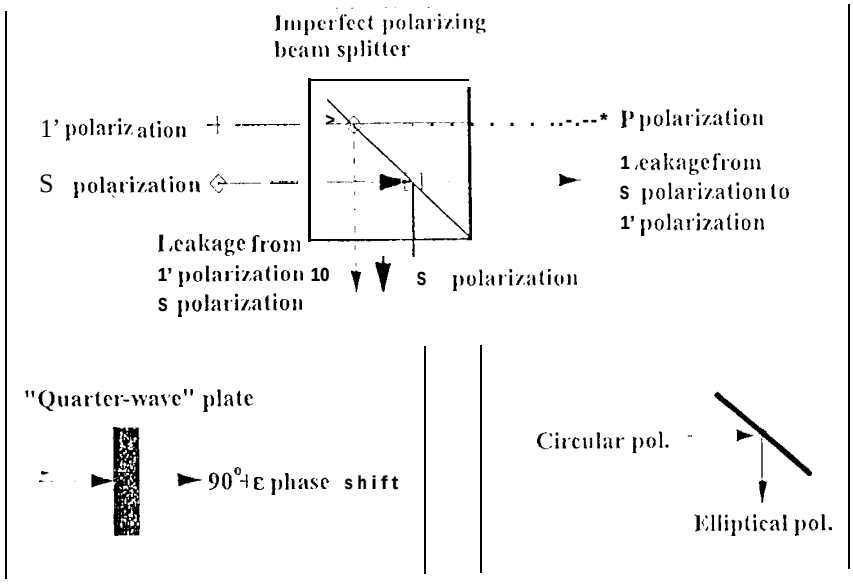

Figure 7: Cyclic averaging

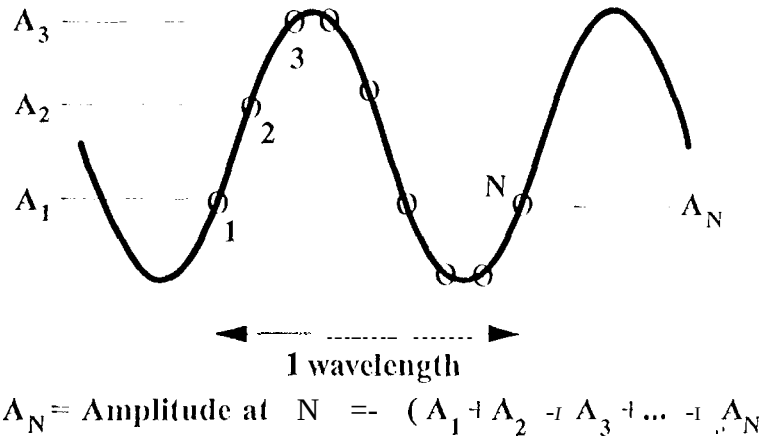

These systematic errors can be classified into two categories: The periodic systematic errors due to the polarization leakage with a period of exactly one wavelength and the systematic errors caused by temperature gradients which appear as a small linear drift over short time scales between the readings of the interferometers. In this paper, we will consider only the periodic systematic errors. The temperature gradient related errors are minimized by actively stabilizing the temperature of various optical components and by performing the relative measurements quickly before a significant drift accumulates.

The periodic systematic errors are eliminated by using a method known as cyclic averaging (Fig. 7). This is implemented by either modulating the distance to be measured with a piezoelectric transducer or by sweeping the laser frequency at a fast rate compared to the changes in the distance being measured. The amplitude of the modulation is chosen to be several wavelengths of light. The output of each interferometer is recorded at a rate to guarantee many readings during one wavelength of motion due to modulation. The true output of tile interferometer at the center of modulation is computed to be the average over one exact wavelength of the modulated readings around the center of modulation.

In the actual experiment, a wavelength is divided in 64 equal parts. The servo is used to advance the distance by one sixty-fourth of a wave at a time while covering several wavelengths. At each step a few seconds of data is collected from the interferometers. The average value of each interferometer reading over this time interval is subtracted from each other. in the absence of any systematic errors, this difference is of the order of few' picometers as determined by the null gauge. Since the laser beams travel through different parts of the optical components, the systematic errors which are present on the interferometer signals are different and do not cancel out when the readings of the two interferometers are subtracted.

Fig. 8 shows the result of cyclic averaging applied to the difference signal between the two interferometers. The data are taken in a c1oscx1 vacuum chamber under atmospheric pressure. After the linear drift is taken out, the residual error is 31 picometers rms.

Fig. 9 shows the same experiment performed under vacuum after cyclic averaging. After the linear drift is taken out, the residual error is 10 picometers rms.

If the amplitude of the self-interfemlce is changing due to various alignment drifts, cyclicly averaging the data mice will not remove all the systematic errors. In this case, the cyclic averaging can be used repeatedly until all systematic errors disappear. The actual gauge signal can be recovered after these integrations provided that the true signal is varying slowly compared to the total integration time.

To illustrate this, consider the following expression representing the difference between the two interferometer signals with non-linearities and drift:

$$\text{Interf}_1 - \text{Interf}_2 = \sum_{i=0}^{N} a_i x^i + \sum_{j=0}^{M} \left(\sum_{k=0}^{L} b_{jk} x^k \right) \sin(2j\pi x) \tag{1}$$

where a_i and b_{jk} are constants. x is the distance traveled by the corner cube with the piezoelectric transducer. The term $\sum_{i=0}^{N} a_i x^i$ represents the drift between the two interferometers and the term $\sum_{j=0}^{M} \left(\sum_{k=0}^{L} b_{jk} x^k \right) \sin(2j\pi x)$ represents the systematic errors with non-linearities and drifting amplitudes.

A typical term containing the systematic errors is of the form $x^k \sin(2j\pi x)$. Cyclically averaging this gives:

$$\int_q^{q+1} x^k \sin(2j\pi x)\, dx = \left(\frac{kq^{k-1} + \text{lower order}}{2j\pi} \right) \cos(2j\pi q) + \frac{k}{2j\pi} \int_q^{q+1} x^{k-1} \cos(2j\pi x)\, dx \tag{2}$$

Note that cyclically averaging once reduces the exponent x^k from k to $k-1$. Hence, after $k+1$ integrations the term $x^k \sin(2j\pi x)$ will vanish. In general, if the highest power in the self-interference term is L, then $L+1$ cyclic averagings are needed to completely remove self-interference.

The term representing the drift can be recovered after these operations. To illustrate this, let $N = 2$ in the drift term. Then,

$$\text{drift} = a_0 + a_1 x + a_2 x^2 \tag{3}$$

After cyclically averaging L times:

$$< \text{drift} >_L = a_0 + (L/2)a_1 + (L/4)(L+1/3)a_2 + (a_1 + La_2)x + a_2 x^2 \tag{4}$$

Therefore, a_2 can be obtained by a fit; a_1 can be obtained using a_2 and the linear coefficient of the fit; a_0 can be obtained using a_2, a_1 and the constant term of the fit.

Fig. 10 shows the difference between the two interferometer signals after radiative thermal shields are installed over the experiment in vacuum. Fig. 11 shows the difference after three cyclic averagings and the removal of linear drift. The residual error is 3.5 picometers rms. The linear drift is 33 picometers per wavelength. In this particular experiment, one wavelength was scanned in 2 minutes using 64 steps.

4. IMPROVED RELATIVE METROLOGY GAUGE

Much of the 3.5 picometers rms error is due to the relative thermal drifts between the two heterodyne interferometers in the relative gauge. In our test, all components of the interferometers including the heat producing acousto-optic modulators are mounted on the same optical bench simulating a measurement system in a small spacecraft. In the tests performed in our previous paper, no external thermal regulation was applied other than the thermal insulation provided by the stainless steel vacuum chamber and elastomer seismic isolation pads inside the chamber.

The improved test configuration is shown in Fig. 12. Entire vacuum chamber is thermally insulated from the ambient air by 2 inches of high density foam. In addition, a radiative thermal shield completely enclosing the relative gauge is installed inside the vacuum chamber. Three temperature sensors are monitoring the temperature of the skin of the chamber, the temperature of the inside radiative shield and the temperature of the optical bench carrying the relative gauge.

In the actual experiment, a wavelength is divided in 64 equal parts. The servo is used to advance the distance by one sixty-fourth of a wave at a time while covering several wavelengths. At each step a few seconds of data are collected from the interferometers and the temperature sensors simultaneously.

Figure 8: Relative metrology with cyclic averaging in air

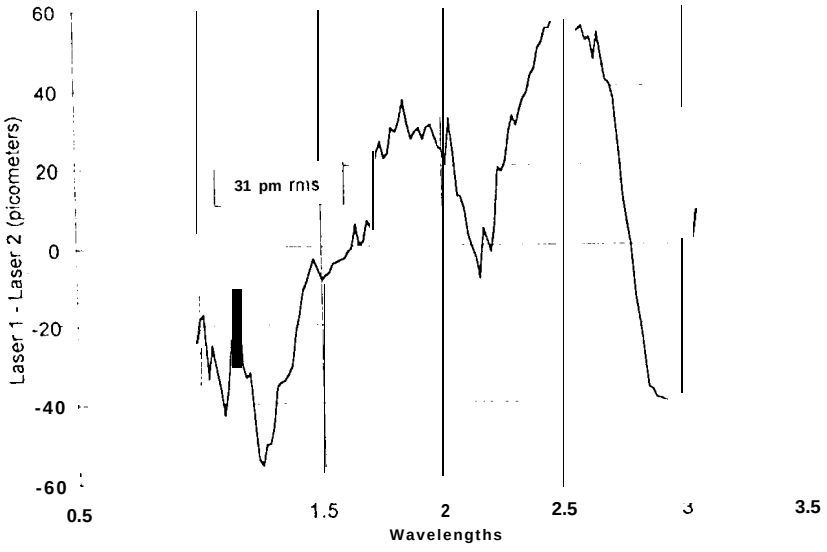

Figure 9: Relative metrology with cyclic averaging in vacuum

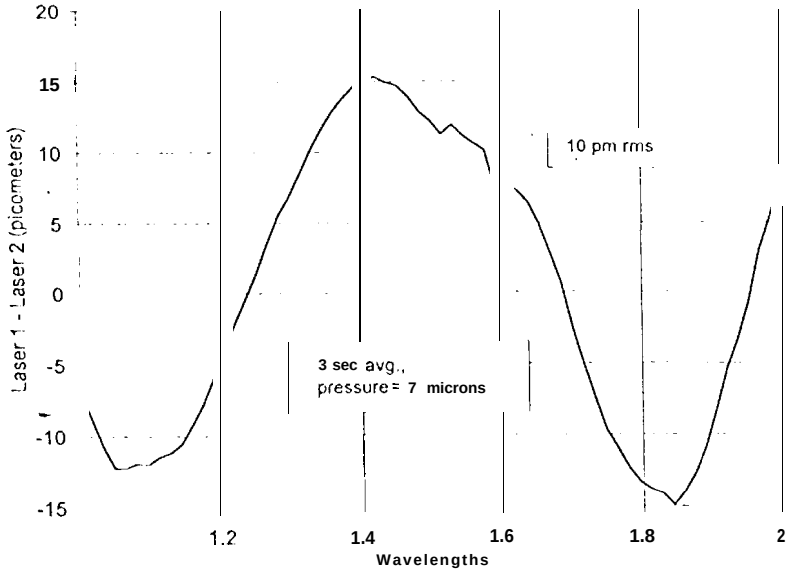

Figure 10: Relative metrology without cyclic averaging in vacuum

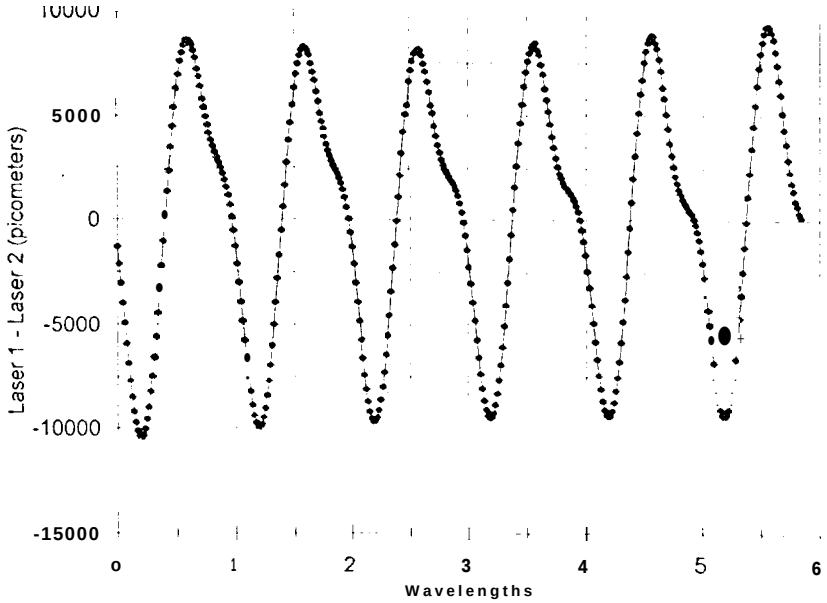

Figure 11: Relative metrology with multiple cyclic averaging in vacuum

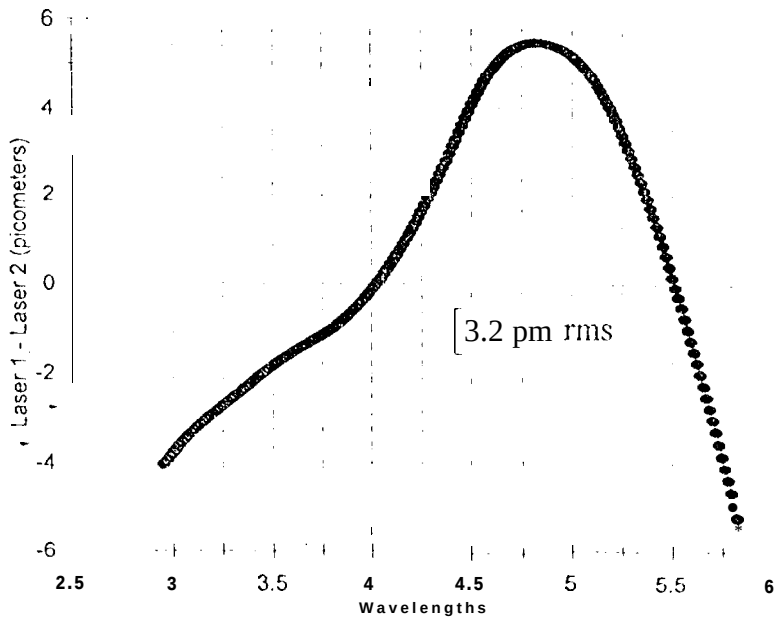

Figure 12: Relative gauge test configuration

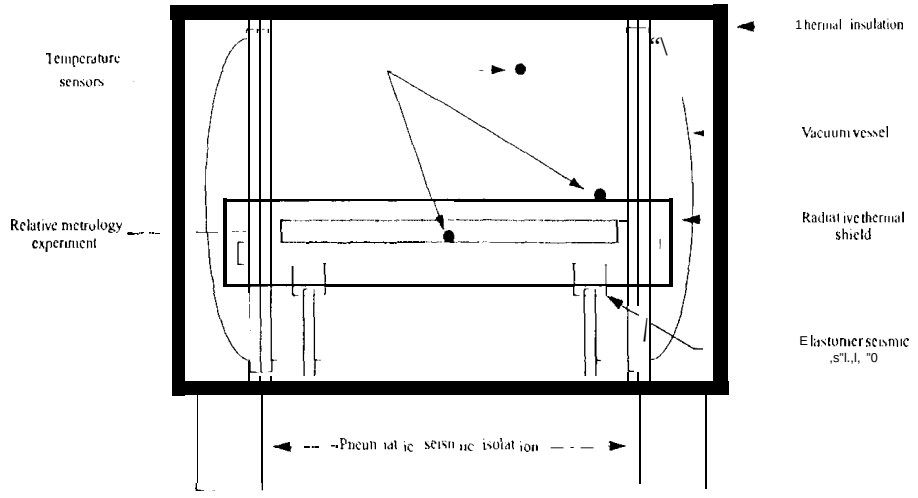

The average value of each interferometer reading over this time interval is subtracted from each other. Since the laser beams travel through different parts of the optical components, the systematic errors which are present cm the interferometer signals are different and do not cancel out when the readings of the two interferometers are subtracted.

The difference data and the temperature data are filtered using the same cyclic averaging filter described in our previous paper. This method eliminates the systematic errors from the interferometer data and computes the average temperature for each cyclicly averaged interferometer data.

The results of the new test of the relative gauge are shown in the following figures. The piezo-electric stack on one of the corner cubes was moved to scan 6 wavelengths at 633 nanometers in few minutes. The average pressure inside the chamber during this test was 5 millitorrs.

Fig. 13 shows the twice cyclicly averaged temperature data from the temperature sensor mounted on the optical bench carrying the relative gauge.

The twice cyclicly averaged relative gauge output corresponding to three separate consecutive sections of the temperature curve are shown in the following figures.

Fig. 14 shows the metrology data taken during the time interval with the smallest change in temperature. The linear drift corresponding to the misalignment of the' interferometers is 3.5 picometers per wave of motion. The residual error is 0.13 pm rms.

Fig. 15 shows the temperature data for the time interval with the smallest temperature change. The temperature stays within 10 millidegrees K of the average temperature.

Fig. 16 shows the metrology data taken just before the stable temperature region. The linear drift corresponding to the misalignment of the interferometers is 23 picometers per wave of motion. The residual error is 1.85 pm rms.

Fig. 17 shows the metrology data taken just after the stable temperature region. The linear drift corresponding to the misalignment of the interferometers is 8 picometers per wave of motion. The residual error is 0.3 pm rms.

The results shove illustrate the sensitivity of the relative gauge to thermal variations. We are implementing an automatic alignment system to keep each interferometer in the relative gauge set-up optimally aligned during operation. The beam launchers of the interferometers arc moved to dither the alignment of each interferometer. From the! collected data, it is possible to compute the the optimal alignment positions of the interferometers. This

Figure 13: Temperature of the optical bench inside the! vacuum vessel

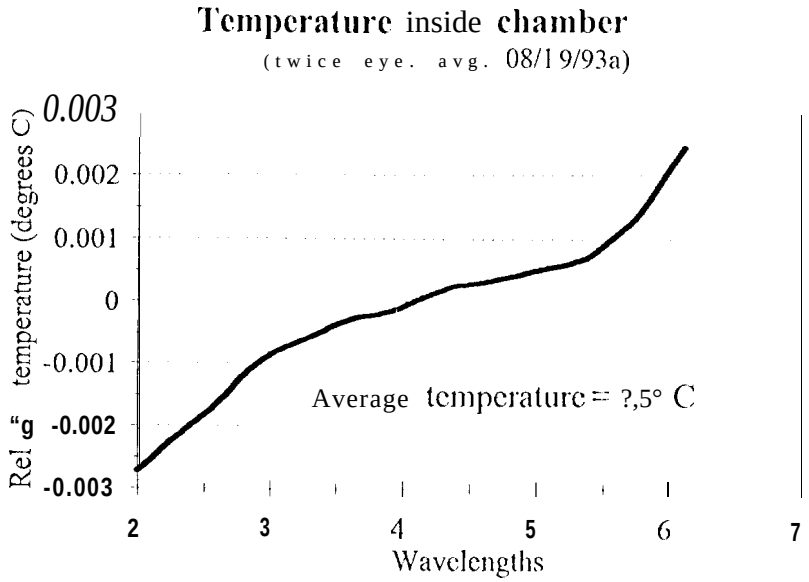

Figure 14: Relative metrology with stable temperature

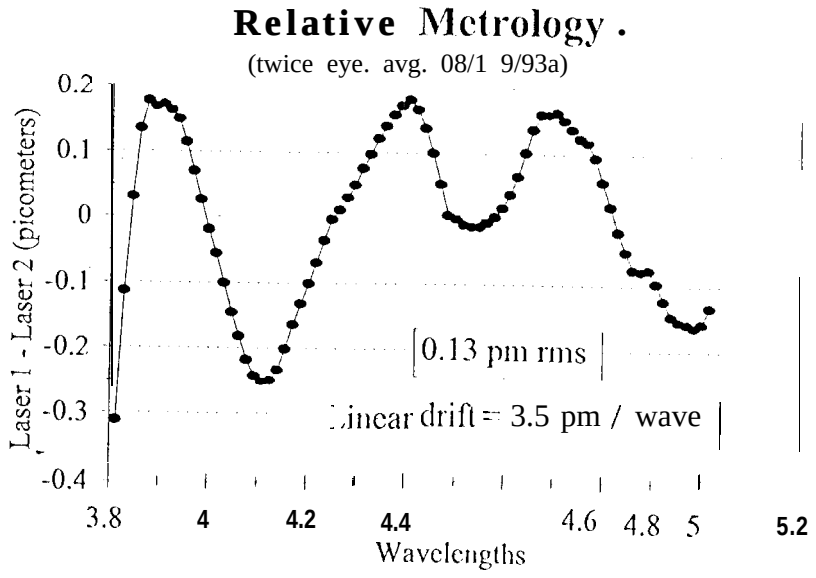

Figure 15: Stable temperature region

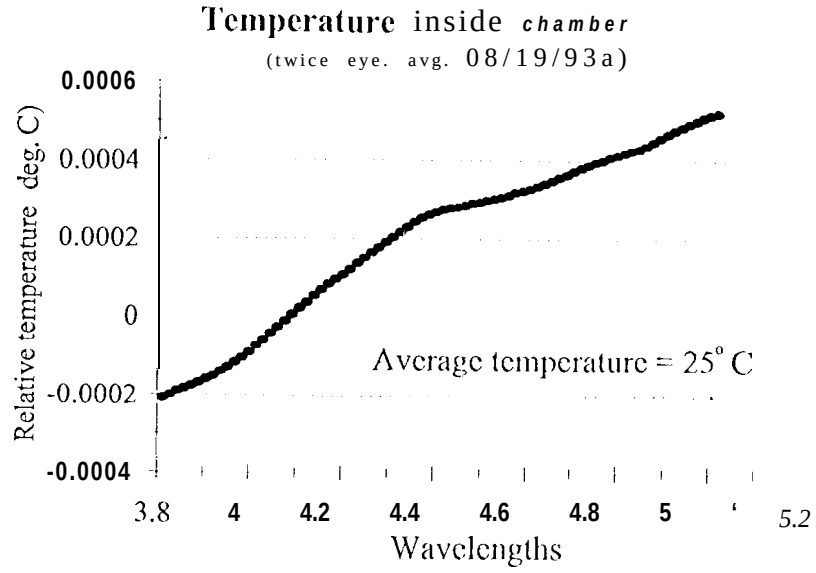

Figure I 6: Relative metrology with less stable temperature (a)

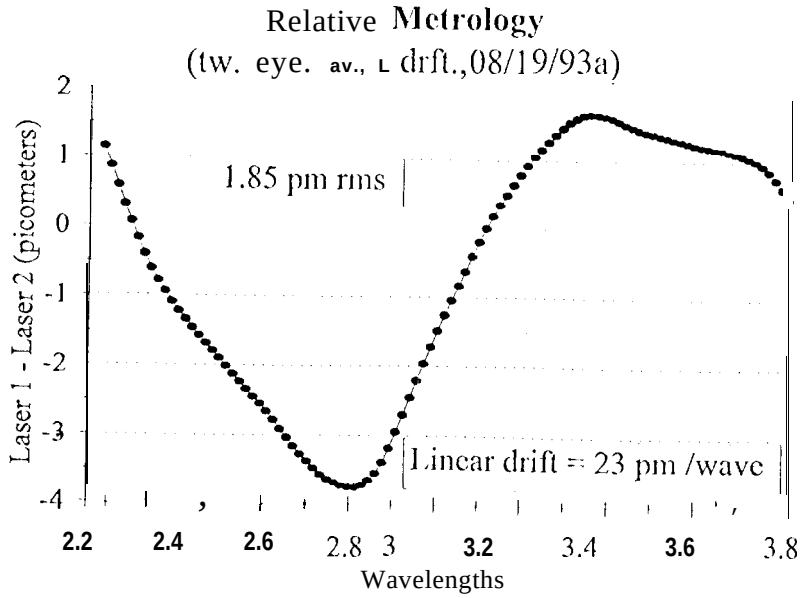

Figure 17: Relative metrology with less stable temperature (b)

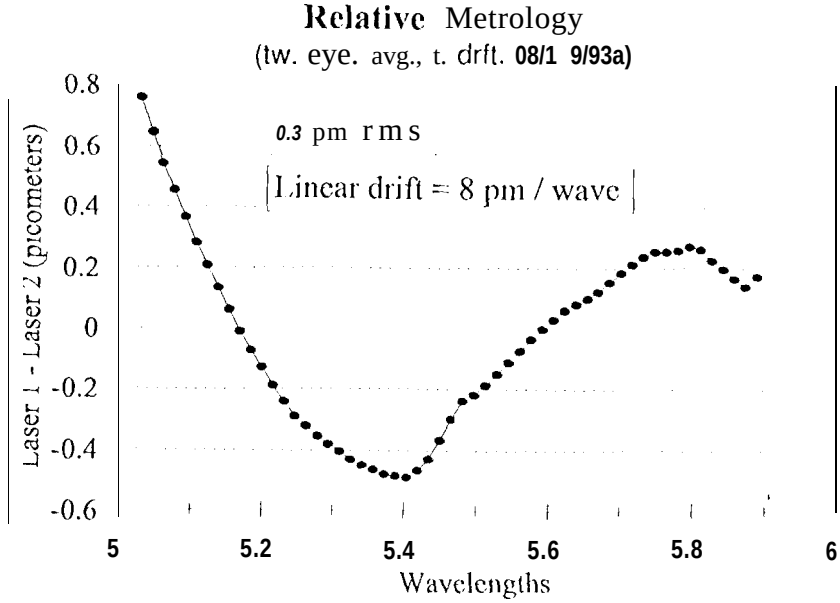

position is parallel to the line connecting the corners of the corner cubes.

A one dimensional interferometer is not capable of detecting transverse motions of these cubes. A three-dimensional relative gauge with five independent auto-aligning, one-dimensional relative gauges is constructed and it is currently being tested.

5. CONCLUSION

The precision and the accuracy of the heterodyne interferometer is improved to sub-picometer level. A faster relative gauge which sweeps the frequency of the laser to implement cyclic averaging is under construction.

6. ACKNOWLEDGEMENTS

I would like to thank M. Shao, M.M. Colavita, J. Yu and B.E. Hines for many fruitful discussions. The research described was performed at the Jet Propulsion Laboratory, California Institute of Technology, under a contract with the National Aeronautics and Space Administration.

7. REFERENCES

1. M. D. Rayman, M.M. Colavita, R. N. Mostert, J. Yu, et al. Orbiting Stellar Interferometer (OSI): FY92 Study Team Progress Report, JPL internal document JPLD-10374, December 14, 1992.

2. M. M. Colavita, M. Shao and M. D. Rayman. "Orbiting stellar interferometer for astrometry and imaging", Applied Optics, Vol. 32, No. 10, p. 1789-1797, 1993.

3. B. Hines, M. Colavita, K. Wallace, A. Poulsen. SUB-NANOMETER LASER METROLOGY SOME TECHNIQUES AND MODELS, *in Proceedings of the High Resolution Imaging by Interferometry II*, Garching, Germany, 1991.

4. Y. Gürsel. Laser metrology gauges for OSI, *in Proceedings Of SPIE conference on Spaceborne Interferometry*, Vol. 1947, p. 188-197, 1993.

5. Y. Gürsel. Metrology for spatial interferometry, *in* Proceedings of *SPIE conference on Amplitude and Intensity Spatial Interferometry*, Ire]. 2200, p. 27-34, 1994.

G. Y. Gürsel. Metrology for spatial interferometry III, *in Proceedings of SPIE conference on Technology in Support of Space Missions*, Vol. *2807*, to be printed in 1996.

CLEARANCE NO. 19

PREPuE3LICATION REVIEW RECORD

INSTRUCTION: Check statement of circumstances applicable to this clearance and indicate action taken.

APPLICABLE CIRCUMSTANCES]:

1. ( ) A JPL "reportable item" is not disclosed but may exist or be "in the making. " (NOTE: Originate Notice of New Technology).

2. (X) JPL or ( ) JPL SubK unreported "reportable item" is disclosed. (NOTE: Originate Notice of New Technology -if SubK. request NTR and decline clearance until NTR is received. Caltech and NMO to review for foreign fling when "item" is within a statutory class of patentable subject matter).

3. ( ) Reported item of new technology is disclosed - U.S. Patent Application filed, (NOTE: Look for reportable and/or patentable improvements. Ask NMO or Caltech for instructions if any are found).

4. ( ) Reported item of new technology is disclosed -no U.S. Application tiled (NOTE: Look for new reportable subject matter for new NTR. If subject matter for new NTR is present, it should be prepared. If a patent application has been ordered or is in preparation, the new subject matter should be brought to the attention of the attorney as soon as possible and foreign filing review bv Caltech and NMO is essential.

5. ( ) JPL SubK invention, of other 3rd party invention, will be disclosed. (NOTE: Deny clearance unless written Permission to publish has been obtained from invention owner).

ACTION TAKEN:

(X) Talked with Y. Gursel Tel. 4-3645

(X) Reviewed: ( ) abstract (x) manuscript ( ) title of publication only.

( ) Notice of New Technology originated - copy of clearance, abstract, manuscript or article put in case folder.

( ) Because this is not a JPL invention, Written permission of invention owner for JPL publication has been confirmed.

(X) Foreign filing Review. Clearance approved by:

9/3/96
NMO Rep. Date

'CIT Rep. ep. Date

CLEARANCE: ( ) Recommended (X) Conditional - see Comments ( ) Delayed - see Comments

COMMENTS: Release conditioned on submittal of an NTR and foreign filing clearance.

PREPARED BY: Linda M Ross
8/30/96